NON-RESONANT VIBRATION ENERGY HARVESTER FOR SUB-HERTZ AND SUB-G VIBRATION

Junyi Wang*, Aobo Zhang, Diana Cantini, and Eun Sok Kim
Department of Electrical and Computer Engineering
University of Southern California, Los Angeles, CA 90089, USA

ABSTRACT

This paper presents a non-resonant vibration energy harvester (VEH) optimized for 0.5-1.0 Hz at 0.2g acceleration, typically associated with human motion in daily activities. Different amounts of water-based and oil-based ferrofluids as liquid bearings have been studied in an experimental setup with a precisely controllable spacing between top and bottom coil plates where the magnet array and ferrofluid bearings reside. The sub-miniature VEH (1.4cc and 3.3gram) steadily generates voltages between 0.5-1.0 Hz and is measured to produce an open-circuit voltage of $V_{\rm rms}=19.5$ - 31.9 mV (or 0.33-0.89 μW into a match load) from 0.2g sub-Hz applied acceleration. The highest figure of merit (FOM) of the VEH at 0.2g at 1.0 Hz is 15.5 $\mu W/cc/g^2$.

KEYWORDS

Vibrational Energy Harvesters, Wearable Devices, Human Motion, Self-power, Sustainable Energy, Power MEMS, Non-Resonant Electromagnetic Energy Conversion, Ferrofluids.

INTRODUCTION

Vibrational electromagnetic energy harvesters can be used to harvest power from human motion [1-3]. However, harvesting power from human motion without loading the person is challenging as the motion is at an extremely low frequency (from sub-Hz to a few Hz), which basically rules out a resonant structure for a vibration energy harvester (VEH) [4]. Even with a non-resonant VEH based on ferrofluid bearing [1], the friction or damping inside the VEH becomes an issue for sub-Hz and sub-g acceleration.

Ferrofluid as a liquid bearing reduces the friction between a magnet array and its supporting plate and was shown to be effective in generating power from human walking motion [1]. A subminiature non-resonant electromagnetic VEH based on ferrofluid bearings [1] was reported to generate 7.6 μW to a matched load from the back of a human walking at 2 m/sec (about 2 Hz), while its improved version [5] increased the figure of merit (FOM) by 20% for 1 g, 2 Hz acceleration. Though ferrofluid bearing is ideal for frictionless support for non-resonant VEHs, the friction and the damping by the liquid bearing can be substantial as the VEH is pushed for higher power generation (e.g., by adding a coil array at the top of the VEH package) and for effective power generation from $0.5-1.0~{\rm Hz}$ with ultra-low acceleration.

This paper presents our study on ferrofluid bearing's impact on friction and damping as a function of the ferrofluid amount, applied acceleration frequency, spacing between the top and bottom coilarray plates, etc. Also presented is a comparison between waterbased and oil-based ferrofluids. Experimental results on a non-resonant VEH optimized for 0.5-1.0 Hz and sub-g acceleration are presented.

DESIGN AND METHODS

Structure Design

As shown in Fig. 1, four N52 NdFeB magnets are assembled to form a linear magnet array with alternating north and south orientations on a planar surface so that magnetic flux changes in the direction parallel to the planar surface may peak at the boundary between two magnets [6]. As the largest magnetic field gradient

appears at the boundaries of the abutting magnets, we place an array of five width-matched coils (of AWG 43 self-bonding copper wire) on the top and bottom of the magnet array (Fig. 1). Each coil array consists of five coils wound by the customized winding machine ACME's AEX-01 around an oval shape spool of 1.5 mm in height, 3.8 mm in the major axis, and 1.1 mm in the minor axis [5]. Top and bottom coil arrays are attached to superhydrophobic plates (made by spraying Rust-Oleum 274232 coating on a 0.5 mm thick acrylic sheet) for water-based ferrofluid or oleophobic plates for oil-based ferrofluid. A coil array is placed on one side of the plate, while the other side supports ferrofluid bearings, which are attracted and selfaligned to the magnet array (Fig. 1). A rectangular chamber formed by two superhydrophobic or oleophobic plates (along with four sidewalls) houses a magnet array inside its enclosed volume while supporting a coil array on its top and bottom faces. The ferrofluid between the magnet array and the superhydrophobic or oleophobic plates reduces the friction greatly, and thus, the friction between the sidewalls and magnets' sides is a main source of the friction for magnet movement after the optimization of the ferrofluid amount. Since the friction is related to the contact area of the sidewalls and magnets, the four sidewalls are recessed for a stepped structure to minimize the contact area.

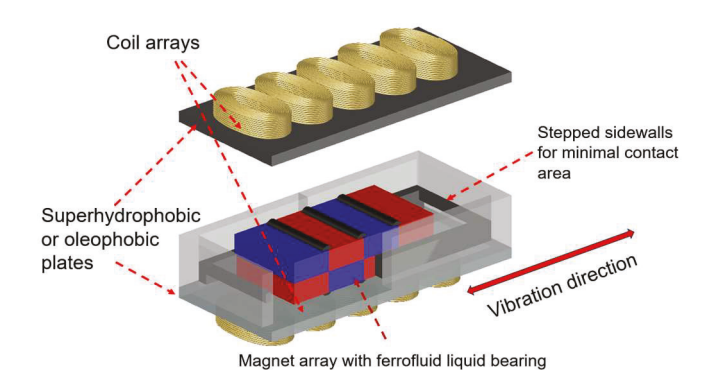


Figure 1: Schematic of the VEH with the magnetic array suspended by ferrofluid bearings (at the top and bottom of the array) with stepped side walls for minimal contact area for minimal friction between side walls and the magnet array.

Based on the size of each magnet being 6.4 mm long and 3.2 mm wide, we match the coil width to 3.2 mm and then cut the superhydrophobic or oleophobic plates to be 18.8 mm long and 6.8 mm wide, providing a magnet array of four magnets with 6.0 mm movable range. The height of the sidewalls will be determined after the height optimization. The VEH size and properties are listed in Table 1.

Optimization Method

The optimization goal is to find the best ferrofluid amount and corresponding chamber height for VEH to generate maximum power at 0.2g and 0.5-1.0 Hz acceleration, which is associated with the human walking motion. The ferrofluids applied on the top and bottom of the magnet array are water-based type EMG 705 and oil-

based type APG 1132 (from FerroTec), whose major properties are listed in Table 2 [7]. Though the oil-based ferrofluid has a much larger viscosity than the water-based one (thus being less effective as a frictionless support for the magnet array), the oil-based ferrofluid dries much slower than the water.

Table 1: Non-resonant VEH optimized for sub-Hz, sub-g vibration.

Total volume and weight	1.4 cc and 3.3 gram		
Magnet Size (mm ³) and Number	6.4 x 3.2 x 3.2 and 4		
Magnet Array's Movable Range	6 mm		
Inner Chamber Size (mm ³)	18.8 x 6.8 x 3.7		
Coil Size (mm ³)	3.2 x 6.4 x 1.8		
Number of Coils Per Coil Array	5		
Total Number of Coil Turns	3,500		
Total Coil Resistance (Ω)	285		

Table 2: Major properties of the ferrofluids.

Туре	Carrier Liquid	Density (g/cc)	Viscosity (mPa·s)	Magnetic Particles
EMG 705	Water	1.19	<5	3.9% vol
APG 1132	Synthetic hydrocarbon oil	1.05	200	11 – 30% vol

A micro-pipette of 3-20 µL range is used to dispense ferrofluids on the surface of the magnet array. The ferrofluids self-assemble at the boundaries of the abutting magnets because of the high magnetic field intensity. With different amounts of ferrofluids applied, the magnet array is placed on a test chamber attached to the platform of a linear actuator Aerotech ACT115DL, whose motion is programmed and controlled by the Soloist Motion Composer software. To optimize the amount of the ferrofluid, we focus on two factors: the relative moving velocity of the magnet array to the chamber and the root mean square (RMS) of the open circuit voltage (V_{RMS}) generated by the bottom and top coil arrays. We capture the slow-motion video of the magnet array moving with the chamber and find the location of the magnet array center. The moving velocity is calculated by the difference of the location of the current frame to the last frame divided by the time of one frame. The maximum relative moving velocity indicates that the corresponding ferrofluid amount is the best amount for VEH to generate the maximum voltage. However, the maximum relative velocity does not necessarily guarantee the maximum V_{RMS} because of the ferrofluid's impact on the magnetic field distribution. Thus, we also measure the V_{RMS} from the bottom and top coil arrays (with the top coil array placed far away from the chamber to exclude the influence of the spacing between the top and bottom coil arrays). Combining the two sets of data, we determine the best amount of ferrofluid to be applied on the top and bottom surfaces of the magnet array.

After finding the optimum ferrofluid amount, we determine the best spacing between the top and bottom coil arrays, as a narrower distance between the coil array and the magnet array gives a higher magnetic flux gradient (which is desirable) but higher friction which hinders the movement of the magnet array. The spacing between the top and bottom coil array is varied with a 3D-micropositioner in an experimental setup that allows the top coil array to be moved up and down precisely, as shown in Fig. 2. Since the height of the magnets is 3.2 mm, the chamber height used in this optimization experiment is 3.2 mm. The lowest tested height is when the magnet array starts to move the full range of the chamber, while the highest tested height is when the top superhydrophobic plate or oleophobic plate loses contact with the top ferrofluid bearing. The optimization is based on the total V_{RMS} of the two coil arrays that are serially connected.

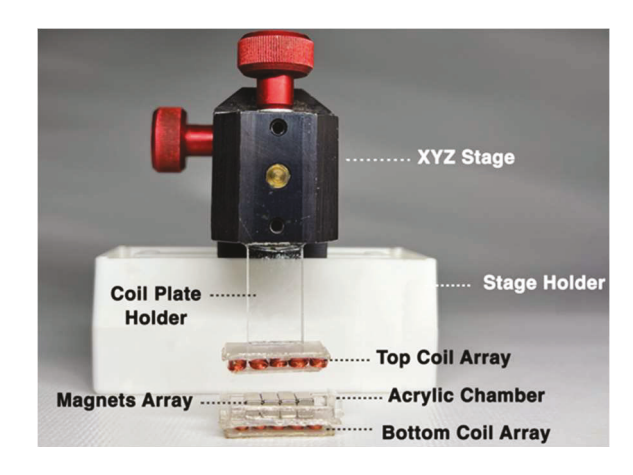


Figure 2: Experimental setup for adjustable spacing between the top and bottom coil arrays for the VEH to optimize the package height.

RESULTS

As the ferrofluid amount on the boundaries of the magnet array is increased, the EMG 705 ferrofluid first fills up the spacing at the boundaries up to about 4 μL per boundary and then covers the north or south surface of the magnet array at around 8 μL per boundary. When the ferrofluid is increased further to 11 μL per boundary, it starts to appear at the opposite surface of the magnet array. In the case of APG 1132, the spacing at the boundaries is filled up at about 4 μL per boundary, and the surface is covered at around 9 μL per boundary. However, even if the ferrofluid is increased beyond 11 μL per boundary, no ferrofluid shows up at the opposite surface due to the high magnetic-particle concentration and viscosity of the oil-based ferrofluid.

The linear actuator (on which the chamber containing the magnet array sits) is driven with a sinusoidal voltage at 0.5 Hz for a peak sinusoidal acceleration of 0.2g. By analyzing the slow-motion videos by Tacker software which is used to track the location of the magnet array center, we measure the relative displacement of the magnet array to the chamber (Fig. 3). For EMG 705, the ferrofluid amount less than 3 µL per boundary is too small for frictionless suspension of the magnet array relative to the chamber, as the chamber moves (Fig. 3a). Ferrofluid amount of 4 - 11 µL per boundary is sufficiently large to suspend the magnet array with little friction over the 6 mm movable range inside the chamber. The relative velocity for 4 - 11 µL (calculated from the same videos) is the highest when 10 µL ferrofluid is applied to each boundary (i.e., 30 µL ferrofluid applied to the surface), as can be seen in Fig. 4a. This indicates that the optimum ferrofluid amount is near 10 µL per boundary, and we narrow the optimization range to 6-12 µL per boundary in measuring the V_{RMS} from the coil arrays. As shown in Fig. 5a, the V_{RMS} reaches its highest voltage with 10 μL per boundary, which is the optimum ferrofluid amount for 0.2g, 0.5 Hz movement. For APG 1132, the ferrofluid amount of less than 5 µL per boundary is too small for frictionless suspension of the magnet array relative to the chamber as the chamber moves (Fig. 3b). Ferrofluid amount of 5 - 14 µL per boundary is sufficiently large to suspend the magnet array with little friction over the 6 mm movable range inside the chamber. However, the relative velocity with oilbased ferrofluid is about half smaller than that with water-based ferrofluid because of >40 times higher viscosity. The relative velocity for 5 - 14 μL is the highest when 11 μL ferrofluid is applied to each boundary (Fig. 4b). The V_{RMS} also is the highest with 11 μ L per boundary (Fig. 5b) but is lower by a factor of about five than the V_{RMS} obtained with water-based ferrofluid. The RMS voltage difference is much greater than the relative-velocity difference, likely due to much higher magnetic particle concentration in the oilbased ferrofluid, as the magnetic particles reduce the magnetic field strength between the magnet array and the coil array.

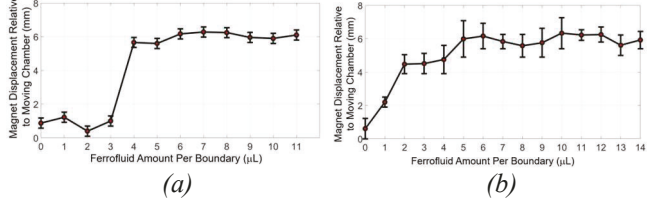


Figure 3: Measured relative displacement range (between the magnet array and the moving package) vs amount of ferrofluid on the bottom side of the magnet array for applied 0.2g sinusoidal acceleration at 0.5 Hz; (a) with EMG 705 and (b) with APG 1132. The magnet array moves inside a chamber having a movable range of 6 mm.

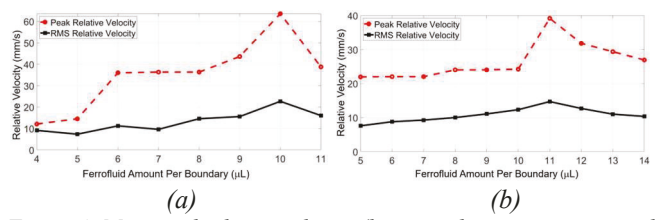


Figure 4: Measured relative velocity (between the magnet array and the moving package) vs amount of ferrofluid on the bottom side of the magnet array for applied 0.2g sinusoidal acceleration at 0.5 Hz, showing the optimum ferrofluid amount of 10 µL per boundary for 0.5 Hz; (a) with EMG 705 and (b) with APG 1132.

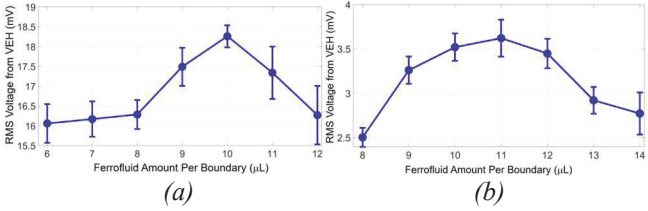


Figure 5: Measured root-mean-square (RMS) voltage vs ferrofluid amount for 0.2g sinusoidal acceleration at 0.5Hz from the bottom and top coil arrays with the top coil array placed far away from the chamber; (a) with EMG 705 and (b) with APG 1132.

The relative velocities are non-sinusoidal for a sinusoidal acceleration (Fig. 6) for both water-based and oil-based ferrofluids and are much less than the velocity associated with the applied acceleration (substantially worse for the VEH with oil-based ferrofluid and for that with water-based). The magnet array supported by water-based ferrofluid (EMG 705) experiences equally high relative velocity during the chamber acceleration and deceleration (with the peak relative velocity being about half of the peak relative velocity of the ideal case of the magnet array being suspended completely frictionless by the ferrofluid bearing, as if it were freely suspended in air [1]). In the case of the magnet array supported by APG 1132, the magnet array moves along with the chamber (and thus almost zero relative velocity) during a half cycle due to the oil's high viscosity. The peak relative velocity is also lower with the oil-based ferrofluid, indicating a magnet-array suspension with much higher mechanical coupling between the magnet array and the support plate via the oil-based ferrofluid.

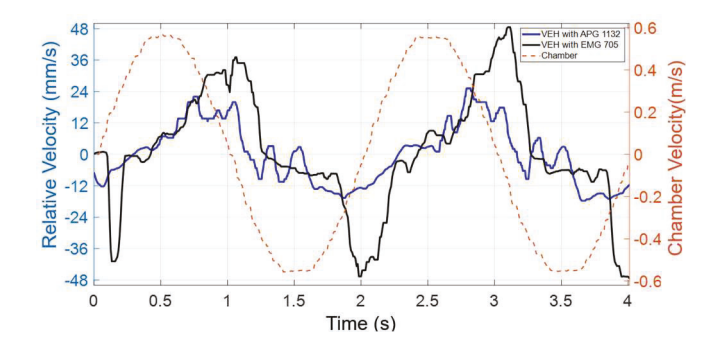


Figure 6: Relative velocities of VEH with 10 µL ferrofluids (APG 1132 or EMG 706) per boundaries versus time as the chamber is moved sinusoidally with a peak acceleration of 0.2g at 0.5 Hz.

Having determined the optimum amount of the ferrofluids, we vary the spacing between the top and bottom coil arrays in a setup shown in Fig. 2. In the case of EMG 705 (water-based ferrofluid), when the spacing is larger than 3.4 mm, the magnet array moves the whole movable range of 6 mm (though with a substantial amount of friction), and the suspension of the magnet array by the ferrofluid works with least amount of the pressing impact by the top and bottom plates. When the spacing is increased to 4.0 mm, the top superhydrophobic surface is separated from the ferrofluid, leaving an air gap between the two. Under the same movement of the linear actuator that moves the chamber, the measured V_{RMS} is the largest when the spacing is 3.7 mm, as can be seen in Fig. 7a. In the case of APG 1132 (oil-based ferrofluid), the measured V_{RMS} is the largest when the spacing is 4.0 mm (Fig. 7b) and is lower by a factor of about five than that for the case of EMG 705 (Fig. 7a).

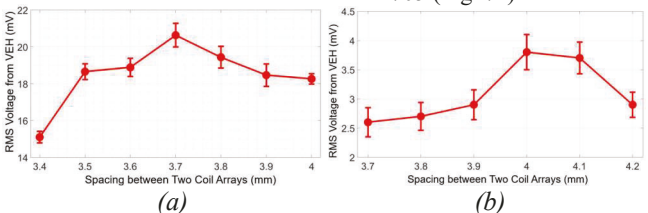


Figure 7: Measured RMS voltage versus the spacing between the two coil arrays for 0.2g sinusoidal acceleration at 0.5Hz with the optimum amount of ferrofluids: (a) with EMG 705 and (b) with APG 1132

The power generation by the optimized VEH (Fig. 8) with water-based ferrofluid (EMG 705) is characterized at 0.2 and 0.25g acceleration over 0.5 - 1.0 Hz and 2 - 4 Hz by measuring the opencircuit V_{RMS}. The measured V_{RMS} for 0.20 and 0.25g versus frequency (Fig. 9) shows that for 0.5 - 1.0 Hz, the generated voltage steadily increases as the frequency increases. However, at 0.20 g acceleration, the generated voltage starts dropping when the frequency is increased beyond 1 Hz because the relative movement range of the magnet array inside the chamber becomes less than the movable range of 6 mm. With the smaller relative movement, the generated voltage starts increasing when the frequency is increased beyond 2 Hz. On the other hand, the drop of the generated voltage at 3 Hz for 0.25g acceleration is because of the critical frequency being 3.5 Hz above which the voltage drops [1]. The generated voltage at 0.25g acceleration is higher than that at 0.20g acceleration, indicating that even though the VEH is optimized for 0.20g acceleration, it can effectively generate power from higher acceleration because of the non-resonant characteristics of the VEH. The figure of merit (FOM) of the VEH is defined as the power delivered to a matched load of 285 (per volume per square of applied

acceleration) and is calculated from the open-circuit voltage. As shown in Fig. 10, the FOM peaks (at 1.0 Hz for 0.20 g acceleration) to be $15.5~\mu W/cc/g^2$ (for power delivered to a matched load of 285Ω), unprecedented for sub-Hz and sub-g VEH. The highest FOM is even higher (23.5 $\mu W/cc/g^2$) for 0.25g acceleration but at 3 Hz.

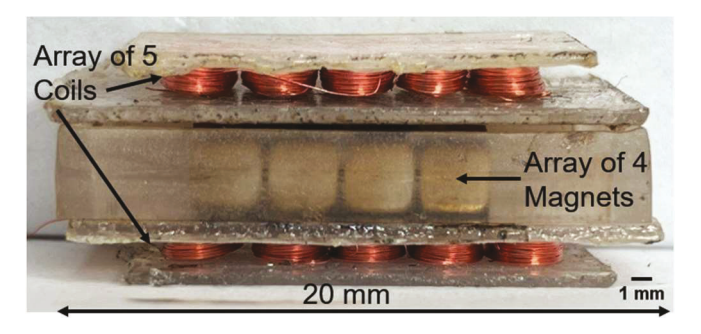


Figure 8: Photo of the VEH of Table 1 with 10 µL ferrofluid at each boundary between two abutting magnets.

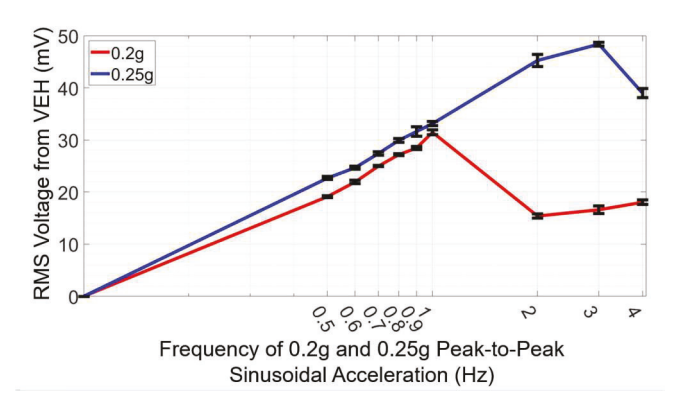


Figure 9: Measured RMS voltages (in linear scale) vs frequency (in log scale) for 0.2g and 0.25g sinusoidal accelerations with the VEH in Table 1 with 10 µL ferrofluid.

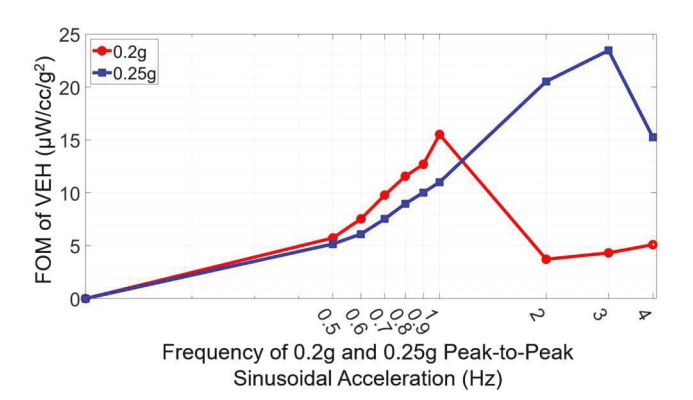


Figure 10: FOM of VEH vs frequency for 0.2g and 0.25g accelerations, showing 15.5 μ W/cc/g² at 1.0 Hz for 0.2g.

At $1.0\,\mathrm{Hz}$, where the FOM is maximum for $0.20\mathrm{g}$ acceleration, we measure the generated voltage vs acceleration over $0.2-1\,\mathrm{g}$ and calculate the FOM, as shown in Fig. 11. The generated voltage steadily increases with the increase of the acceleration, but the FOM drops.

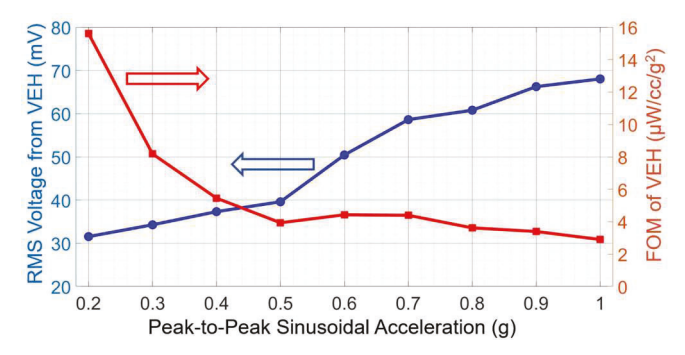


Figure 11: Measured RMS voltage (blue) and FOM (red) vs acceleration amplitude for 1.0Hz sinusoidal acceleration for the optimized VEH.

SUMMARY

This paper describes the optimized non-resonant VEH through optimization of the (1) ferrofluid amount and (2) the spacing between top and bottom coil arrays for 0.2g, 0.5 Hz acceleration. The optimum amount of water-based ferrofluid applied to each boundary of the magnet array turns out to be 10 μL , with which the relative velocity and generated voltage both are the best, while the optimum spacing is measured to be 3.7 mm. The optimized VEH (1.4 cc and 3.3 gram) is measured to generate voltage with a maximum FOM as high as 15.5 $\mu W/cc/g^2$ for 1.0 Hz, 0.2g acceleration.

ACKNOWLEDGEMENTS

This paper is based on the work supported by the National Science Foundation under grant ECCS-1911369.

REFERENCES

- [1] Y. Wang, Q. Zhang, L. Zhao and E.S. Kim, "Non-Resonant, Electromagnetic Broad-Band Vibration-Energy Harvester Based on Self-Assembled Ferrofluid Liquid Bearing," IEEE/ASME Journal of Microelectromechanical Systems, vol. 26, no. 4, pp. 809 – 819, 2017.
- [2] Q. Zhang, Y. Wang, E.S. Kim, "Power generation from human body motion through magnet and coil arrays with magnetic spring" J Appl Phys, 115 (2014)
- [3] Liu, Huicong, et al. "A non-resonant rotational electromagnetic energy harvester for low-frequency and irregular human motion." Applied Physics Letters 113.20 (2018).
- [4] Uematsu, Azusa, et al. "Preferred step frequency minimizes veering during natural human walking." Neuroscience Letters 505.3 (2011): 291-293.
- [5] M. Barekatain, J. Wang, A. Roy, K. Sadeghian Esfahani, J. Lee and E.S. Kim, "Non-Resonant Vibration Energy Harvester with Wound Micro-Coil Arrays," Transducers '23, The 22nd International Conference on Solid-State Sensors, Actuators and Microsystems, Kyoto, Japan, June 25 - 29, 2023, pp. 1272 - 1275.
- [6] Q. Zhang and E.S. Kim, "Vibration Energy Harvesting Based on Magnet and Coil Arrays for Watt-Level Handheld Power Source," Proceedings of the IEEE, vol. 102, no. 11, pp. 1747 – 1761, 2014.
- [7] https://ferrofluid.ferrotec.com/

CONTACT

*J. Wang, tel: +1-323-768-4872; junyiw@usc.edu